

--- Supporting Information ---

^{17}O MAS NMR Correlation

Spectroscopy at High Magnetic Fields

Eric G. Keeler^{1,§}, Vladimir K. Michaelis^{1,†}, Michael T. Colvin^{1,‡}, Ivan Hung², Peter L. Gor'kov², Timothy A. Cross², Zhehong Gan², and Robert G. Griffin^{1,*}

⁽¹⁾ Department of Chemistry and Francis Bitter Magnet Laboratory, Massachusetts Institute of Technology,
Cambridge, Massachusetts, 02139 USA

⁽²⁾ National High Magnetic Field Laboratory, Florida State University, Tallahassee, FL 32310

§ - Current Address: Department of Chemistry, Columbia University, New York, NY, 10027 USA

† - Current Address: Department of Chemistry, University of Alberta, Edmonton, Alberta, T6G 2G2

Canada

‡ - Current Address: Ortho Clinical Diagnostics, Rochester, NY, 14626 USA

*Corresponding Author: Robert G. Griffin, rgg@mit.edu

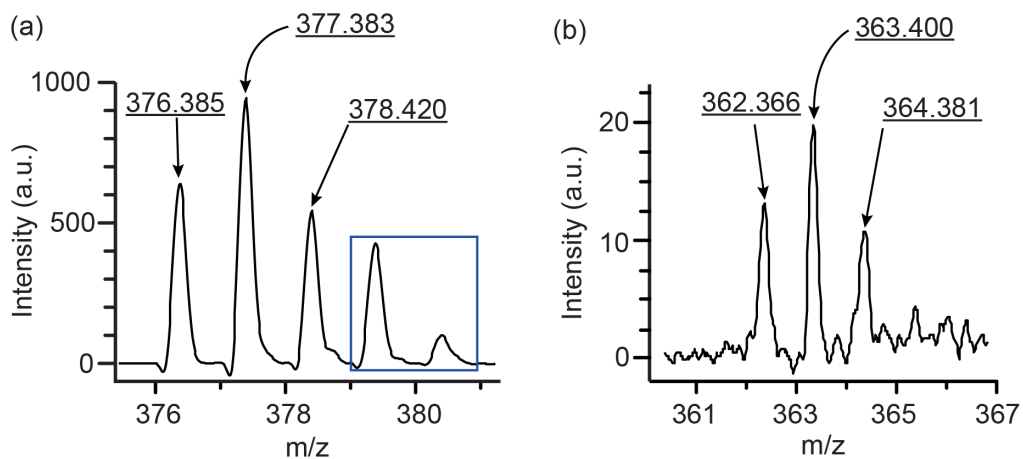


Figure S1: MALDI mass spectra of 40% - ^{17}O labeled Fmoc-L-leucine (a) and Fmoc-L-valine (b). The blue box in (a) is due to the alpha-cyano background from the MALDI matrix. The isotopic enrichments were calculated by taking the integrated peak intensities of the $^{16}\text{O}/^{16}\text{O}$ species as 0%, the $^{16}\text{O}/^{17}\text{O}$ species as 50%, and the $^{17}\text{O}/^{17}\text{O}$ species as 100% enrichment.

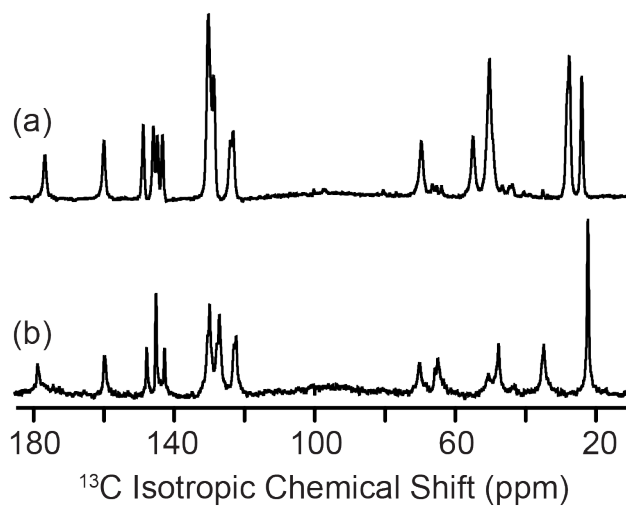


Figure S2: $^{13}\text{C}\{^1\text{H}\}$ CPMAS NMR spectra of Fmoc-L-leucine (a) and Fmoc-L-valine (b) at 11.7 T ($\omega_{\text{OH}}/2\pi = 500$ MHz) with $\omega_{\text{R}}/2\pi = 10$ kHz and $\gamma B_1/2\pi = 100$ kHz ^1H TPPM decoupling.

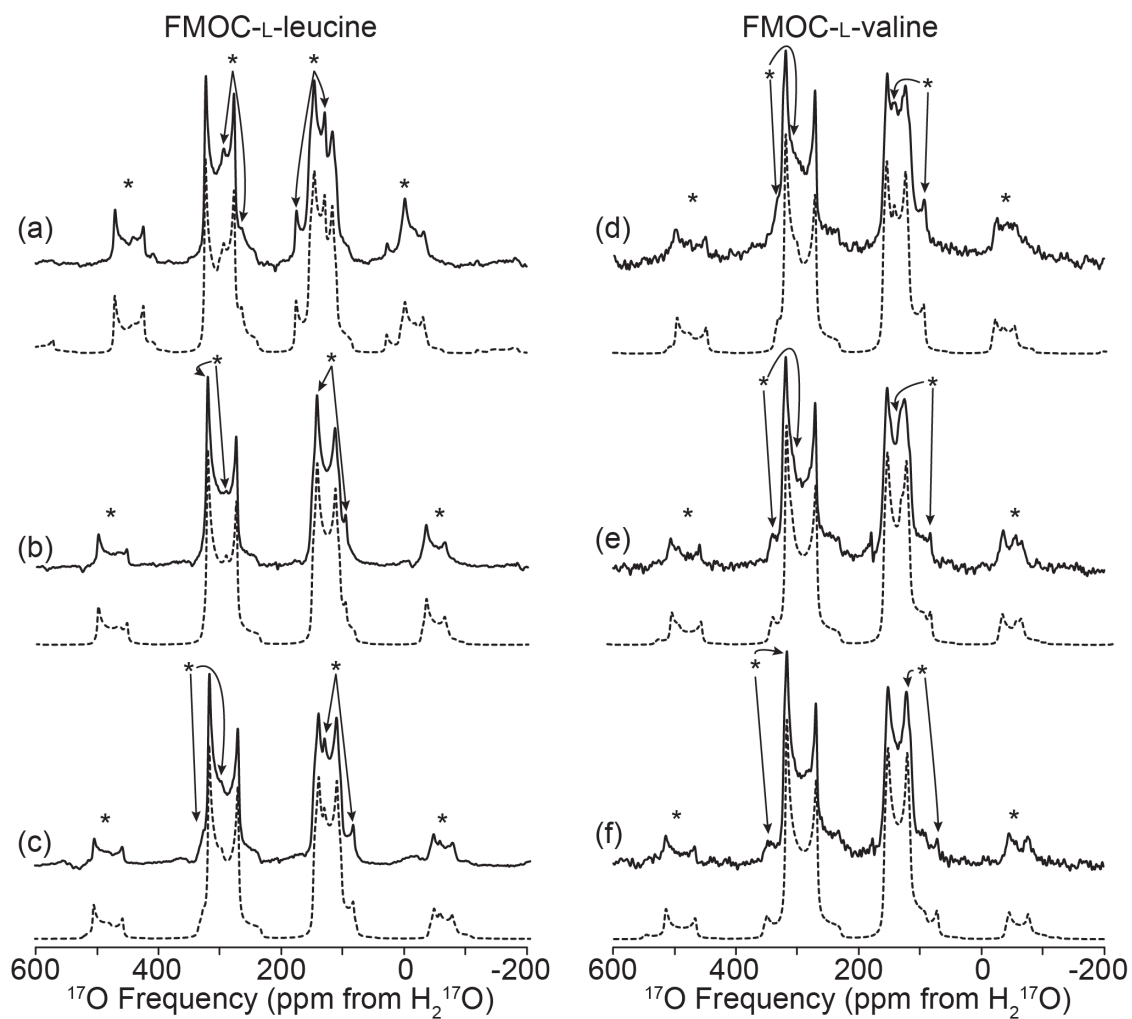


Figure S3: Oxygen-17 experimental (solid) and simulated (dashed) MAS NMR spectra of FMOC-L-leucine (right) and FMOC-L-valine (left) at 17.6 T ($\omega_{0H}/2\pi = 750$ MHz). $\omega_R/2\pi = 15$ kHz (a), $\omega_R/2\pi = 17$ kHz (b), $\omega_R/2\pi = 18$ kHz (c) for FMOC-L-leucine and $\omega_R/2\pi = 18$ kHz (d), $\omega_R/2\pi = 19$ kHz (e), $\omega_R/2\pi = 20$ kHz (f) for FMOC-L-valine. Spinning sidebands are noted by astericks (*). NMR parameters used in spectral simulations are given in Table 4.

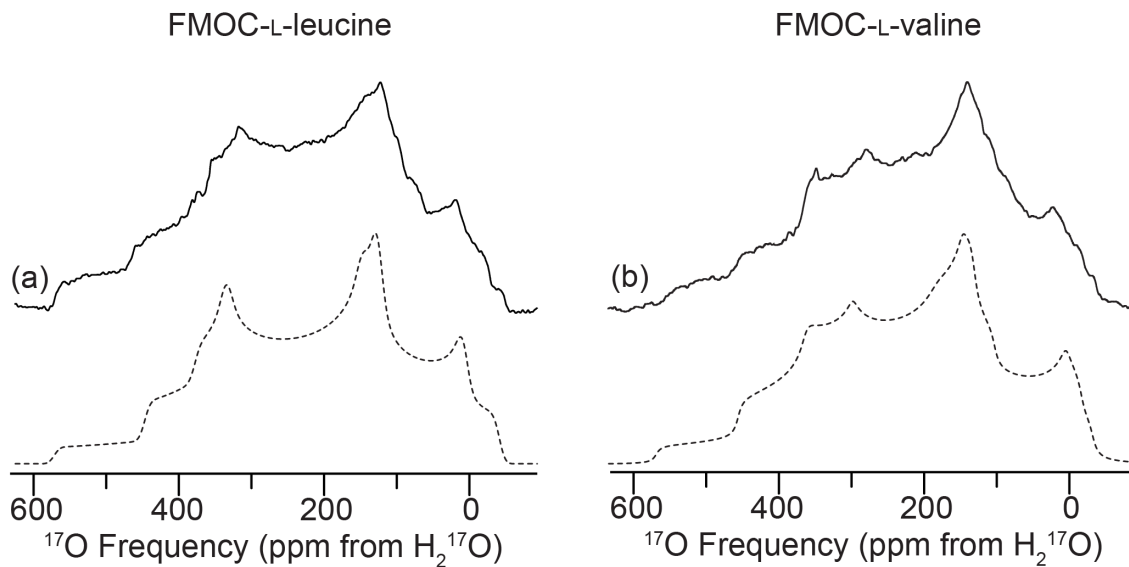


Figure S4: Oxygen-17 experimental (solid) and simulated (dashed) non-spinning NMR spectra of FMOC-L-leucine (a) and FMOC-L-valine (b) at 17.6 T ($\omega_{0H}/2\pi = 750$ MHz) with $\gamma_{B1}/2\pi = 100$ kHz continuous-wave 1H decoupling. NMR parameters used in spectral simulations are given in Table 4.

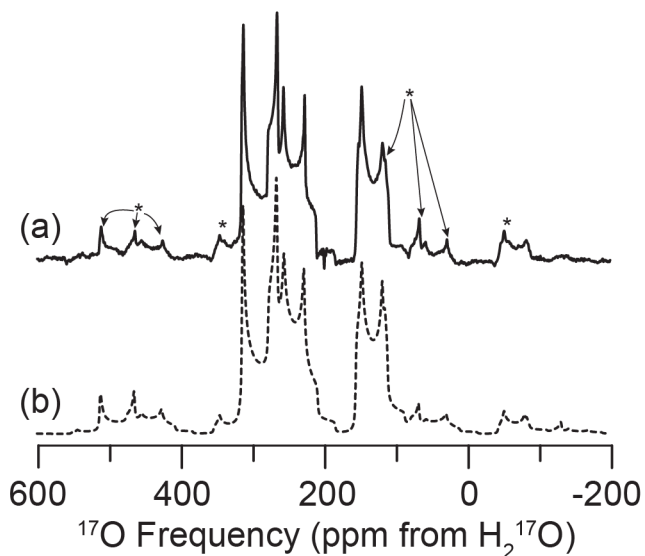


Figure S5: Oxygen-17 MAS NMR spectrum of N-Ac-VL (a), simulation of MAS NMR spectrum (b) at 17.6 T ($\omega_{0H}/2\pi = 750$ MHz). Spectra were acquired with $\omega_R/2\pi = 20$ kHz, spinning sidebands are noted by asterisks (*). NMR parameters used in spectral simulations are given in Table 4.

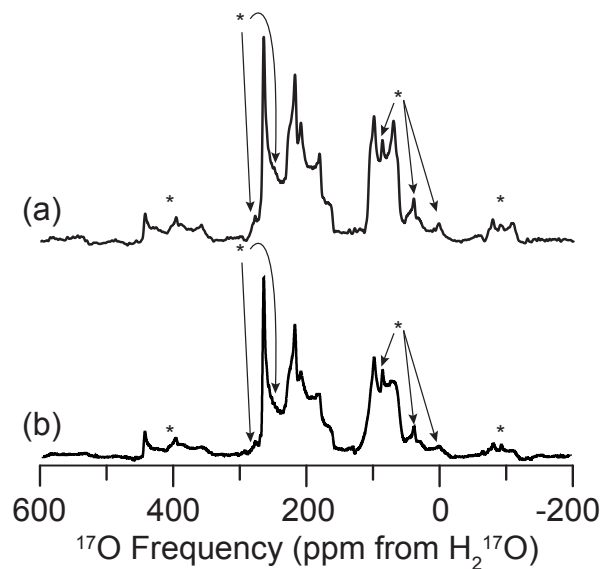


Figure S6: Oxygen-17 MAS NMR spectrum of N-Ac-VL without (a), and with (b) $\gamma B_1/2\pi = 100$ kHz continuous-wave ^1H decoupling at 17.6 T ($\omega_{0\text{H}}/2\pi = 750$ MHz). Spectra were acquired with $\omega_{\text{R}}/2\pi = 18$ kHz, spinning sidebands are noted by asterisks (*).

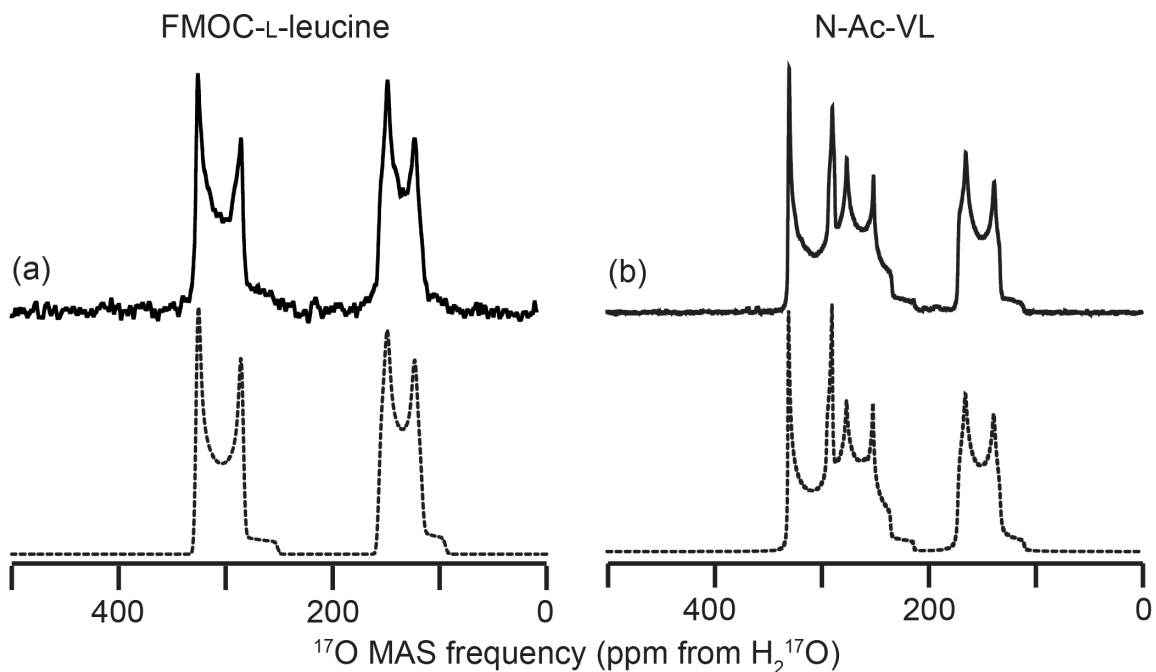


Figure S7: Experimental (solid) and simulated (dashed) ^{17}O MAS NMR of FMOC-L-leucine (a) and N-Ac-VL (b) at 18.8 T ($\omega_{0\text{H}}/2\pi = 800$ MHz). Spectra were acquired with $\omega_{\text{R}}/2\pi = 60$ kHz. NMR parameters used in spectral simulations are given in Table 4.

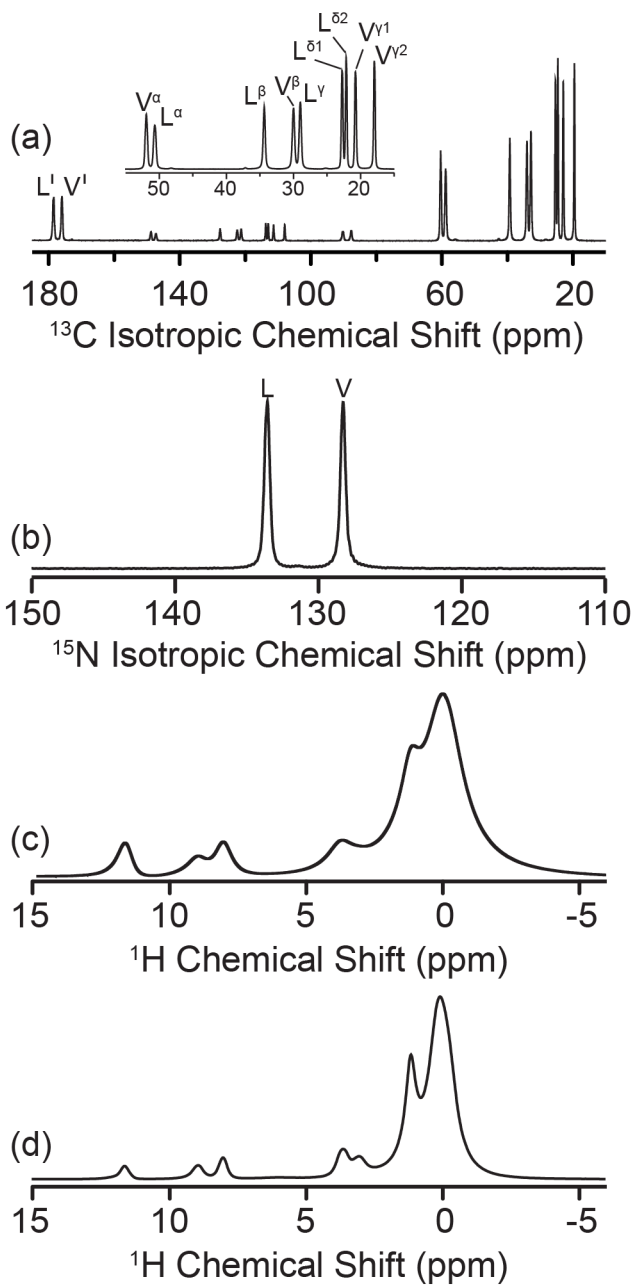


Figure S8: ^{13}C , ^{15}N , and ^1H MAS NMR of N-Ac-VL at 21.1 T ($\omega_{\text{OH}}/2\pi = 900$ MHz) with $\omega_{\text{R}}/2\pi = 20$ kHz. $^{13}\text{C}\{^1\text{H}\}$ CPMAS NMR spectrum (a), $^{15}\text{N}\{^1\text{H}\}$ CPMAS spectrum (b), and ^1H MAS NMR spectrum (c). ^1H MAS NMR spectrum at 18.8 T with $\omega_{\text{R}}/2\pi = 60$ kHz (d). Compared to previous NMR studies of N-Ac-VL.¹⁻³

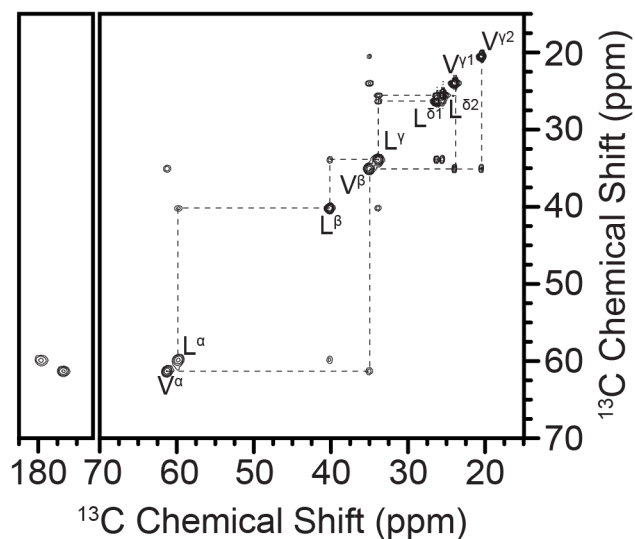


Figure S9: Two-dimensional ^{13}C - ^{13}C RFDR spectrum with 1.6 ms mixing at 11.7 T ($\omega_{0\text{H}}/2\pi = 500$ MHz) and $\omega_{\text{R}}/2\pi = 10$ kHz with $\gamma B_1/2\pi = 100$ kHz continuous wave ^1H decoupling during evolution and $\gamma B_1/2\pi = 100$ kHz TPPM ^1H decoupling during acquisition. Compared to previous study of N-Ac-VL.²

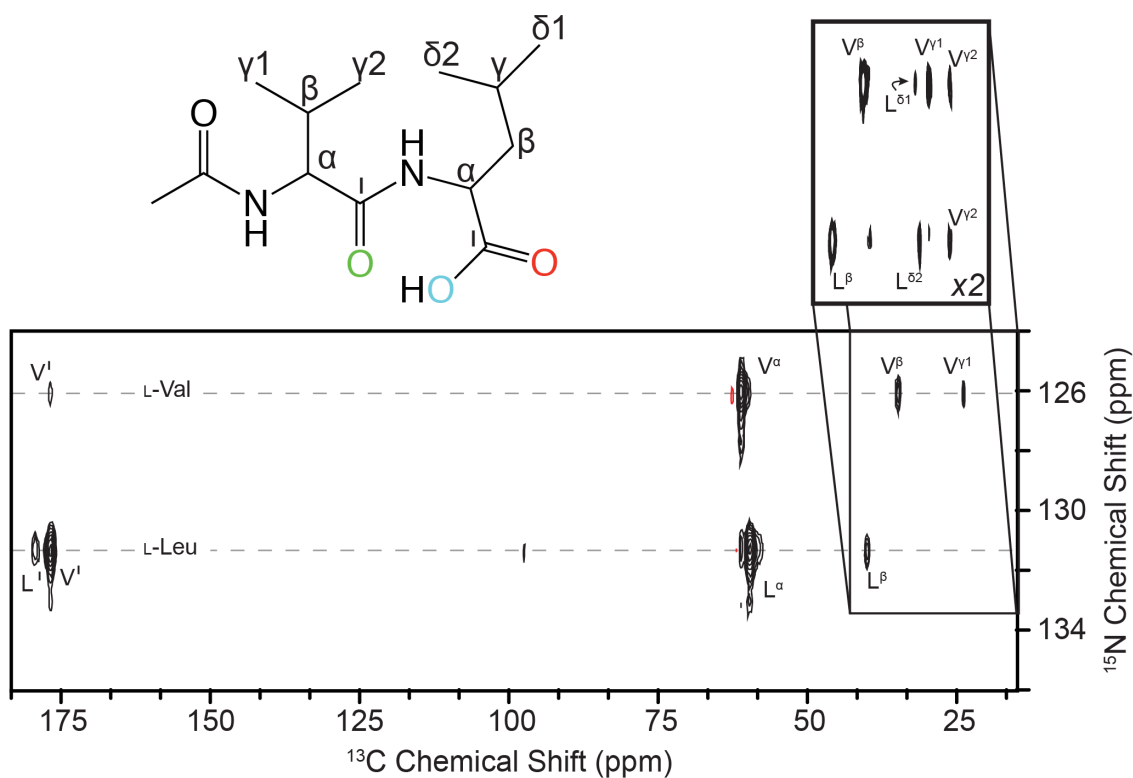


Figure S10: Two-dimensional ^{13}C - ^{15}N ZF-TEDOR spectrum with 2.0 ms mixing at 11.7 T ($\omega_{0\text{H}}/2\pi = 500$ MHz) and $\omega_{\text{R}}/2\pi = 10$ kHz with $\gamma B_1/2\pi = 100$ kHz TPPM ^1H decoupling during acquisition. Compared to previous study of N-Ac-VL.²

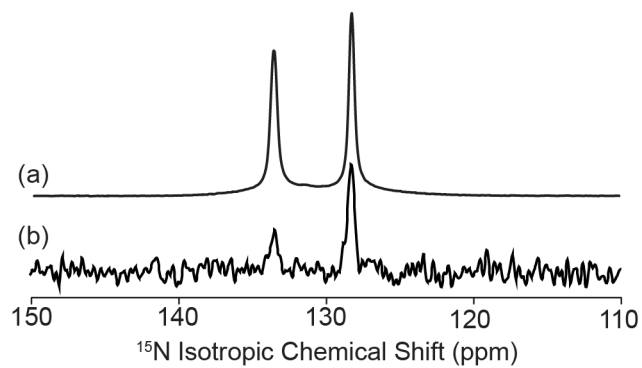


Figure S11: Comparison of 1D ^{15}N CPMAS (a) and ^{15}N - ^{17}O ZF-TEDOR with 7.88 ms of mixing (b) at 17.6 T ($\omega_{\text{OH}}/2\pi = 750$ MHz). Spectra acquired with $\omega_{\text{R}}/2\pi = 18$ kHz, ^{15}N $\gamma\text{B}_1/2\pi = 36$ kHz, and ^1H $\gamma\text{B}_1/2\pi = 100$ kHz TPPM decoupling.

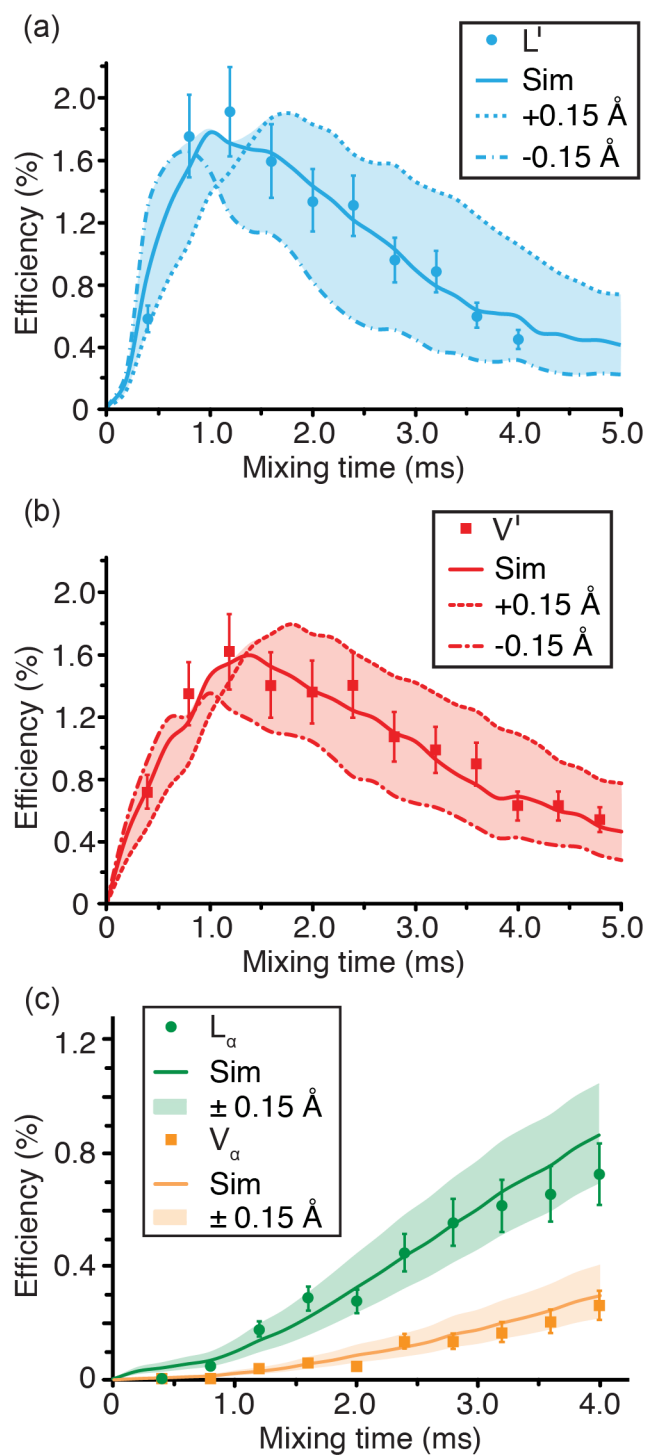


Figure S12: Experimental and simulated, including ± 0.15 Å errors, 1D ^{13}C - ^{17}O ZF-TEDOR buildup curves as a function of mixing time for leucine C' (a), valine C' (b), and Ca (leucine, green circles and valine, yellow squares) (c), at 21.1 T ($\omega_{\text{OH}}/2\pi = 900$ MHz) with $\gamma_{\text{B1}}/2\pi$ (^{17}O) = 100 kHz, and 100 kHz TPPM ^1H decoupling during acquisition. Best fit simulated curves (solid lines) determined using SPINEVOLUTION.⁴ Measured ^{13}C - ^{17}O distances given in Table 5.

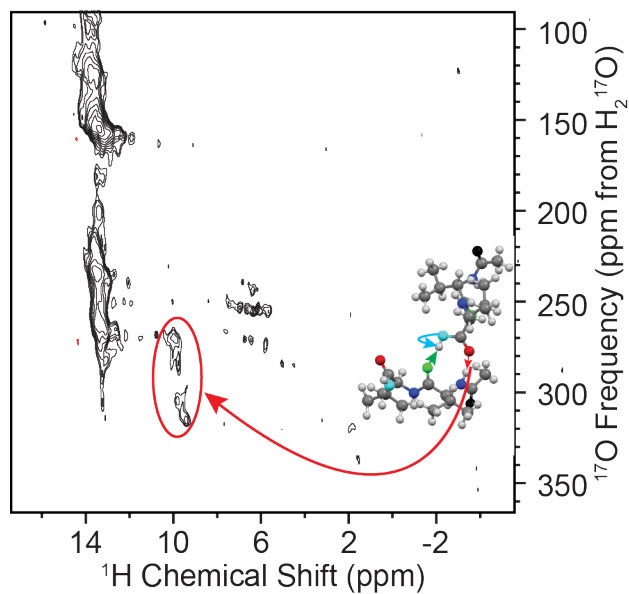


Figure S13: Two-dimensional ^1H - ^{17}O R^3 -R-INEPT spectrum with $R^3 = 100 \mu\text{s}$. Spectra were acquired with $\omega_R/2\pi = 20 \text{ kHz}$ at 17.6 T ($\omega_{0\text{H}}/2\pi = 750 \text{ MHz}$). The correlation, circled in red, between the leucine amide proton to the leucine CO oxygen (red arrow) is indicated on the crystal structure of N-Ac-VL in the inset.⁵

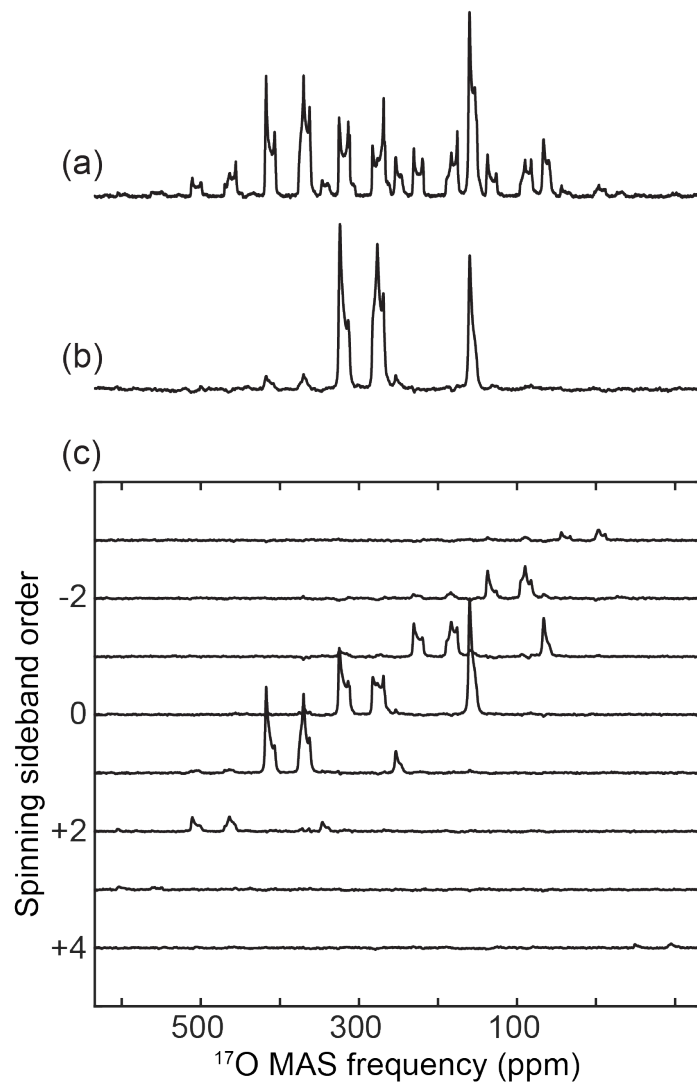


Figure S14: Experimental ^{17}O MAS NMR spectra of N-Ac-VL (a) at 35.2 T ($\omega_{\text{OH}}/2\pi = 1500$ MHz) with $\omega_{\text{R}}/2\pi = 19$ kHz. Sum projection of the ^{17}O MAS NMR spectrum of N-Ac-VL (b) after shearing transform of the direct dimension of the MATPASS spectrum to yield an axis that is equivalent to an infinite spinning frequency MAS spectrum. Two-dimensional ^{17}O MATPASS spectrum of N-Ac-VL (c) showing the centerband of each oxygen chemical environment for each sideband order.

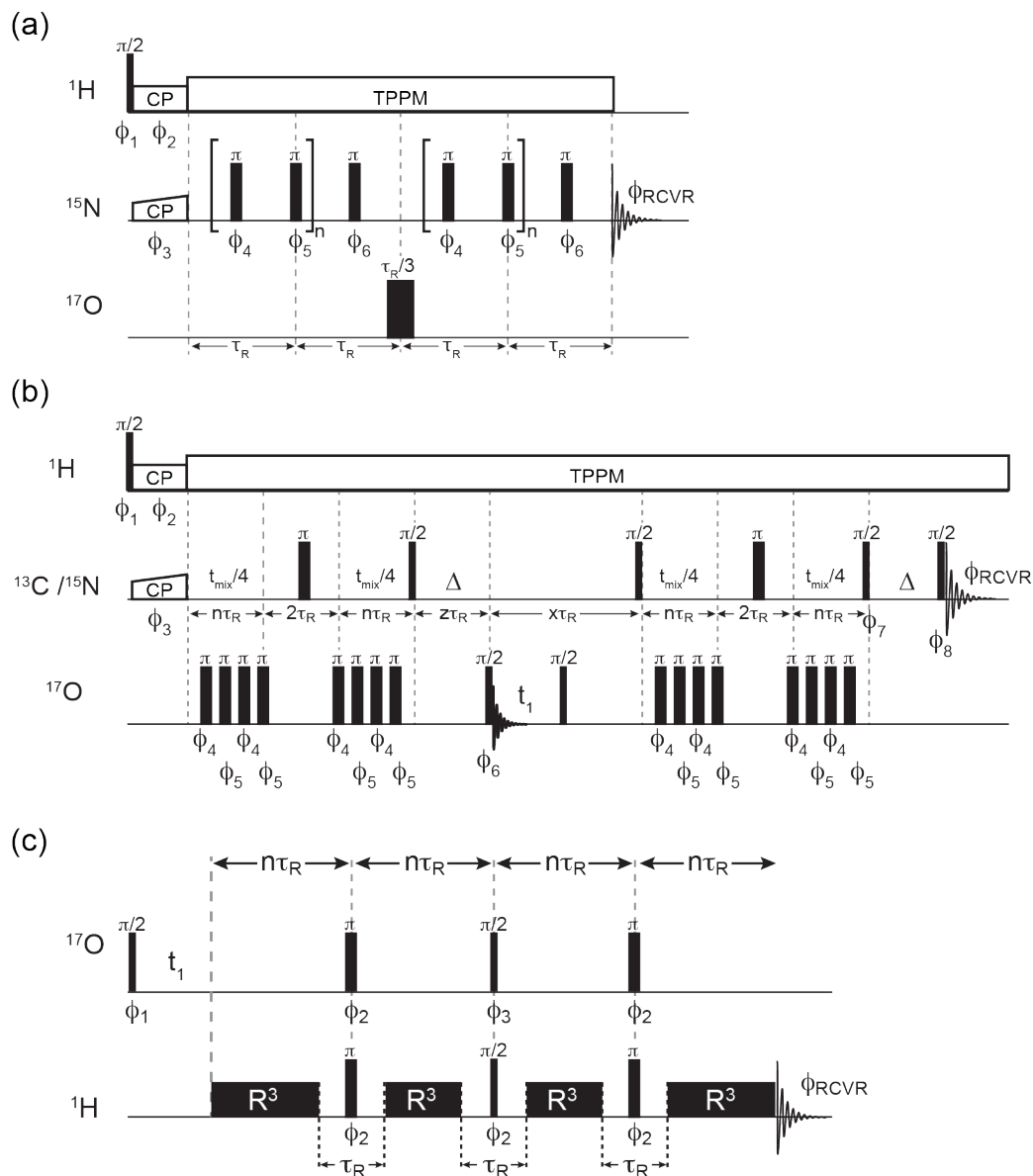


Figure S15: Pulse sequences utilized for correlation experiments. ^{15}N - ^{17}O REAPDOR pulse sequence (a), the phase cycle was: $\phi_1 = 13, \phi_2 = 1, \phi_3 = 1133\ 2244, \phi_4 = 1, \phi_5 = 2, \phi_6 = 1133\ 2244, \phi_{\text{RCVR}} = 1331\ 2442$. $^{15}\text{N}/^{13}\text{C}$ - ^{17}O ZF-TEDOR pulse sequence (b), the phase cycle was: $\phi_1 = 13, \phi_2 = 1, \phi_3 = 2, \phi_4 = 1, \phi_5 = 2, \phi_6 = 13, \phi_7 = 2244, \phi_8 = 1111\ 2222\ 3333\ 4444, \phi_{\text{RCVR}} = 4224\ 1331\ 2442\ 3113\ 2442\ 3113\ 4224$. ^1H - ^{17}O R^3 - R -INEPT pulse sequence (c), the phase cycle was: $\phi_1 = 1234, \phi_2 = 1, \phi_3 = 2, \phi_{\text{RCVR}} = 3412$.

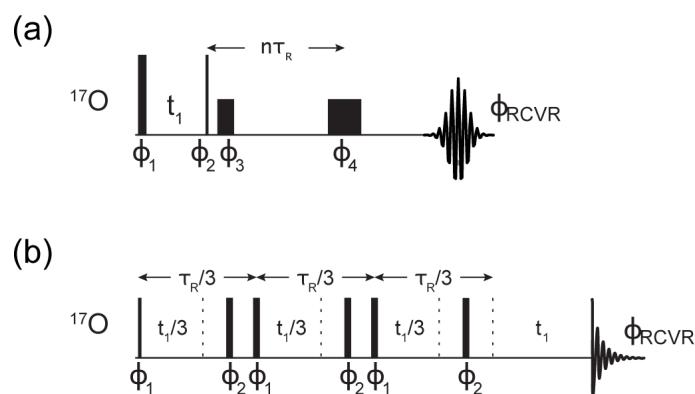


Figure S16: Pulse sequences utilized for ^{17}O NMR experiments at 1500 MHz (^1H). Oxygen-17 3QMAS sequence (a), the phase cycle utilized: $\phi_1 = 0^\circ, 30^\circ, 60^\circ, 90^\circ, 120^\circ, 150^\circ, 180^\circ, 210^\circ, 240^\circ, 270^\circ, 300^\circ, 330^\circ$; $\phi_2 = 0^\circ$; $\phi_3 = 0^\circ$; $\phi_4 = (0^\circ)*12, (45^\circ)*12, (90^\circ)*12, (135^\circ)*12, (180^\circ)*12, (225^\circ)*12, (270^\circ)*12, (315^\circ)*12$; $\phi_{\text{RCVR}} = 1432\ 1432\ 1431\ 2143\ 2143\ 2143\ 3214\ 3214\ 3214\ 4321\ 4321\ 4321$. ^{17}O MATPASS pulse sequence (b), the phase cycle utilized was a 12-step cogwheel phase cycle: $\phi_1 = 1$; $\phi_2 = 0^\circ, 30^\circ, 60^\circ, 90^\circ, 120^\circ, 150^\circ, 180^\circ, 210^\circ, 240^\circ, 270^\circ, 300^\circ, 330^\circ$; $\phi_{\text{RCVR}} = 1\ 3$.

References

1. Jaroniec, C. P.; Filip, C.; Griffin, R. G., *J. Am. Chem. Soc.* **2002**, *124*, 10728-10742.
2. Jaroniec, C. P.; Tounge, B. A.; Herzfeld, J.; Griffin, R. G., *J. Am. Chem. Soc.* **2001**, *123*, 3507-3519.
3. Reif, B.; Jaroniec, C. P.; Rienstra, C. M.; Hohwy, M.; Griffin, R. G., *J. Magn. Reson.* **2001**, *151*, 320-327.
4. Veshtort, M.; Griffin, R. G., *J. Magn. Reson.* **2006**, *178*, 248-282.
5. Carroll, P. J.; Stewart, P. L.; Opella, S. J., *Acta Crystallogr., Sect. C: Cryst. Struct. Commun.* **1990**, *46*, 243-246.